ACS APPLIED MATERIALS & INTERFACES

Research Article

www.acsami.org

# High Selective Performance of Designed Antibacterial and Anticancer Peptide Amphiphiles

Cuixia Chen,[†] Yucan Chen,[†] Cheng Yang,[†] Ping Zeng,[†] Hai Xu,*[,†] Fang Pan,[‡] and Jian Ren Lu*[,‡]

[†]Centre for Bioengineering and Biotechnology, China University of Petroleum (East China), 66 Changjiang West Road, Qingdao 266580, China

[‡]Biological Physics Laboratory, School of Physics and Astronomy, University of Manchester, Schuster Building, Manchester M13 9PL, United Kingdom

Supporting Information

**ABSTRACT:** Short designed peptide amphiphiles are attractive at killing bacteria and inhibiting cancer cell growth, and the flexibility in their structural design offers a great potential for improving their potency and biocompatibility to mammalian host cells. Amino acid sequences such as $G(IIKK)_nI\text{-}NH_2$ ($n \geq 3$) have been shown to be membrane lytic, but terminal amino acid modifications could impose a huge influence on their performance. We report in this work how terminal amino acid modifications to $G(IIKK)_3I\text{-}NH_2$ influence its $\alpha$-helical structure, membrane penetrating ability, and selective actions against different cell types. Deletion of an N-terminal Gly or a C-terminal Ile did not affect their antibacterial activity much, an observation consistent with their binding behavior to negatively charged membrane lipid monolayers. However, the cytotoxicity against mammalian cells was much worsened by the N-terminal Gly deletion, consistent with an increase in its helical content. Despite little impact on the antibacterial activity of $G(IIKK)_3I\text{-}NH_2$, deletion of both terminal amino acids greatly reduced its antitumor activity. Cholesterol present in tumor cell membrane-mimic was thought to constrain $(IIKK)_3\text{-}NH_2$ from penetrating into the cancerous membranes, evident from its lowest surface physical activity at penetrating model lipid membranes. On the other hand, its low toxicity to normal mammalian cells and high antibacterial activity *in vitro* and *in vivo* made it an attractive antibacterial agent. Thus, terminal modifications can help rebalance the different interactions involved and are highly effective at manipulating their selective membrane responses.

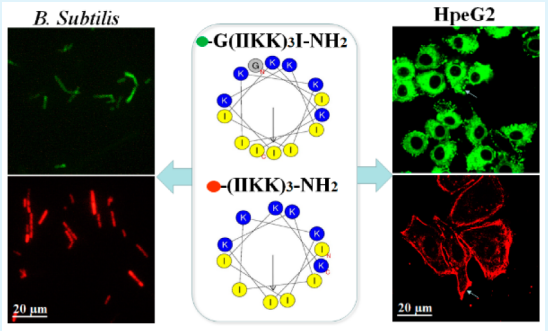


**KEYWORDS:** *helical peptide, surface pressure, membrane penetration, antibacterial peptide, cell selectivity*

## 1. INTRODUCTION

Antibiotic resistance is posing a serious and growing problem to global health. Inappropriate and irrational use of antibiotics has already caused the emergence and spreading of multidrug resistant (MDR) bacteria across many different regions worldwide. New antimicrobial drugs and biocides with working mechanisms different from those of traditional antibiotics and conventional hygiene actives are in great demand.[1−3] Antimicrobial peptides (AMPs) mainly achieve their functions to kill invading microorganisms via nonreceptor-mediated membrane disruptions.[4−6] This physical membrane disruption mechanism results in a lower likelihood for microorganisms to raise their resistance as it becomes metabolically costlier to repair their membrane structures within the typical action periods of minutes.[4,7] AMPs thus hold great promise in new antibiotic development.

As one of the most widely distributed and easily synthesized AMPs, $\alpha$-helical antimicrobial peptides ($\alpha$AMPs) have been extensively investigated, focusing on biomimetic $\alpha$AMPs of certain natural peptide sequences by amino acid replacements, deletions, and modifications by D-amino acids, $\beta$-amino acids, and fluorinated amino acids.[8−13] Furthermore, some minimalist amphipathic peptides have also been *de novo* designed by using bioinformatics and combinatorial libraries.[10,14−16] Terminal modifications could well work as a simple strategy in the design of short $\alpha$AMPs. Modifications at the N- and C-termini could improve the stability of helical structures, resulting in $\alpha$AMPs being less susceptible to enzymatic hydrolysis and high salt strength *in vivo*.[17]

Common terminal modifications include N-terminal acetylation and C-terminal amidation, and it has been demonstrated that both N-acetylation and C-amidation of short lactoferrin-derived hexamers became more stable in human serum than the peptides without any terminal modification.[18] It was also found that ≥70% of natural $\alpha$AMPs start with glycine ($Gly^1$) in their sequences providing resistance to aminopeptidases.[8] Additionally, incorporating Gly at the N-terminus was thought to prevent $\alpha$AMPs from losing their helicity or "unraveling" within pathogenic cells.[19] Substitution of $Gly^1$ with Ala in Fallaxin would greatly reduce its antibacterial activity due to

Received: May 25, 2015
Accepted: July 23, 2015
Published: July 23, 2015





DOI: 10.1021/acsami.5b04547
ACS Appl. Mater. Interfaces 2015, 7, 17346−17355

destabilization to the helix capping.[20] Furthermore, deleting $Gly^1$ of a wild-type influenza hemagglutinin fusion peptide (HA WT-23aa) caused a complete loss of the fusion activity and the reduction of the $\alpha$-helix content from 47% to below 10%, while increasing the $\beta$-sheet structure.[21] However, early studies also indicated that deleting the $Gly^1$ of melittin would improve the antimicrobial activity and hemolytic activity by increasing the content of the peptide helicity.[22] Taken together, N-terminal amino acids, especially $Gly^1$, appear to have different effects on the actions of AMPs associated with its different influences on the secondary structures with different actions on cell membranes, but there is currently a lack of understanding about the exact roles that different amino acids play when used for N-terminal modifications.[21]

In addition to the above N-terminal modifications, hydrophobic modifications with the bulky hydrophobic amino acids such as Trp at the C-terminus could also affect their antibacterial activity.[23] Removal of four amino acids from the C-terminal end of buforin II resulted in a complete loss of its antimicrobial activity because of an reduction of helical content.[24] Similar effects were also found in the designed $[RLLR]_5$ peptide, which contains the helix-capping motifs at the N-terminus (APKAM) and the C-terminus (LQKKGI).[25] Thiol modifications (Cys) at both termini of the designed helical peptides could also enhance antimicrobial activity and selectivity, leading to the effective eradication of clinically isolated multiple drug resistant bacteria.[26]

Despite many reports on the N- and C-terminal modifications of AMPs and their influences on antibacterial activities, no consensus has been reached on the relationship among antibacterial activity, cell selectivity, and terminal modifications, especially on the effects of the terminal modifications with single amino acids. $G(IIKK)_3I\text{-}NH_2$, one of the well-known designed helical peptides, was found to have high activity against MDR extended-spectrum $\beta$-lactamase (*ESBL*)-producing bacteria and tumor cells, while displaying low toxicity to the normal host cells.[27−29] For such a short peptide amphiphile, it is well expected to have large influences from deletion and substitution of terminal amino acids on the secondary structures, but it remains unknown how such structural changes affect antimicrobial activity and various membrane lytic responses. This study has been undertaken to examine the effects of deletion of Gly at the N-terminus and Ile at the C-terminus on the antibacterial and antitumor activity of $G(IIKK)_3I\text{-}NH_2$. The physicochemical characters such as hydrophobicity, surface activity, and secondary structures were measured, and these results were assessed against their antibacterial, antitumor, and hemolytic activities. The insight gained from this work would help us to understand how terminal modifications can be used to design short peptides with greater antimicrobial activity and less cytotoxicity to mammalian host cells.

## 2. MATERIALS AND METHODS

**2.1. Chemical Reagents.** Rink amide-methylbenzhydrylamine hydrochloride salt (MBHA) resin, 9-fluorenyl-methoxycarbonyl (Fmoc) protected amino acids, and other chemicals and solvents used for peptide synthesis were bought from GL Biochem Ltd. (Shanghai). Calcein-AM, phospholipids (eggPC, eggPG), cholesterol, MTT (3-(4,5-dimethyl-2-thiazolyl)-2,5-diphenyl-2*H*-tetrazolium bromide), and other reagents were purchased from Sigma Chemical Co (St. Louis, MO). All chemical reagents were used as received unless otherwise specified. Water used in all experiments was processed with a Millipore Milli-Q system (18.2 MΩ cm).

**2.2. Bacteria, Tumor Cells, and Cultures.** Gram-negative bacteria ($G^-$) used were *Escherichia coli* (*E. coli BL21*) and *ESBL*-producing *Escherichia coli* (*ESBL-E. coli*), and Gram-positive bacteria ($G^+$) used were *Bacillus subtilis* 168 (*B. subtilis* 168) and *Staphylococcus aureus* (*S. aureus*). *E. coli BL21*, *B. subtilis* 168, and *S. aureus* were obtained from China Center of Industrial Culture Collection (Beijing). *ESBL-E. coli* was a gift from Professor Xiaoxing Luo (Department of Pharmacology, School of Pharmacy, Fourth Military Medical University, Xi'an 710032, People's Republic of China). *E. coli BL21* and *ESBL-E. coli* were grown in LB medium (tryptone 10 g/L, yeast extract 5 g/L, NaCl 10 g/L, pH 7.0). *B. subtilis* 168 and *S. aureus* were incubated in beef extract peptone medium (glucose 60 g/L, beef extract 10 g/L, peptone 10 g/L, yeast extract 10 g/L, NaCl 5 g/L, pH7.2).

Tumor cells used were HeLa and HpeG2 cells. They were both purchased from Shanghai Institute for Biological Sciences, and were cultured at 37 °C under 5% $CO_2$ atmosphere in IMDM medium (Gibco, Gland Island, U.S.) containing 10% heat-inactivated fetal bovine serum (FBS). Human blood cells were isolated from the fresh blood of healthy volunteers by centrifuging at 1000 rpm for 20 min at room temperature.

**2.3. Peptide Synthesis and Purification.** $G(IIKK)_3I\text{-}NH_2$ and $FITC\text{-}G(IIKK)_3I\text{-}NH_2$ were synthesized by using a standard Fmoc-based solid-phase method on a commercial CEM Liberty microwave synthesizer. The synthesis and purification procedures were described in detail in our previous studies.[27] The other peptides with different terminal modifications were synthesized following the same procedures. Their purities and molecular weights were determined by reversed phase high performance liquid chromatography (RP-HPLC) and matrix-assisted laser desorption/ionization mass spectrometry (MALDI-TOF MS), respectively. $Rhodamine\text{-}(IIKK)_3\text{-}NH_2$ was purchased from China Peptides Co., Ltd. (Shanghai, China). Each peptide was dissolved in 10 mM saline phosphate buffer (PBS, pH 7.4) at a concentration of 2 mM, and then sterilized by a 0.22 $\mu$m filter. The stock solutions were subsequently frozen and kept at −20 °C until use.

**2.4. Circular Dichroism (CD).** CD spectra were measured on a Bio-Logic MOS 450 spectrometer using a quartz cell of 1 mm path length. Spectra were recorded from 190 to 250 nm at a scan speed of 50 nm/min. Each peptide (2 mM) studied was diluted in water and sodium dodecyl sulfate (SDS) aqueous solution before testing. In all samples, peptide concentration was fixed at 0.1 mM, and the final concentration of SDS was 25 mM. Baseline spectra for each solvent were obtained beforehand. All measurements were carried out at least three times independently at room temperature, and the CD data were expressed as mean residual molar ellipticity $[\theta]$ (deg $cm^2$ $dmol^{-1}$).

**2.5. Antibacterial Assay, Antitumor Activity, and Hemolytic Activity.** Antibacterial activities of the peptides were performed by the standard microdilution method.[27] Briefly, the bacteria from the exponential growth phase were washed twice with PBS and resuspended in the medium. 100 $\mu$L ($1 \times 10^6$ CFU/mL) of bacteria in medium was mixed with 100 $\mu$L of PBS, each containing the peptide in serial reduced dilutions by a factor of 2 in a sterile 96-well plate. The bacteria were incubated at 37 °C for 18 h, and the absorbance at 600 nm was then recorded by using the Molecular Devices (SpectraMax $M^2e$). MIC (minimum inhibitory concentration) was defined as the lowest peptide concentration that inhibits the growth of bacteria after incubation for 18 h.

MTT assay was used to test the antitumor activity of the designed peptides. Briefly, the tumor cells ($1 \times 10^5$ cells/mL) were preincubated for 24 h in a sterile 96-well plate, and then the peptides with a serial of reduced dilutions by a factor of 2 were added into the wells. After incubation with the peptides for 24 h, 20 $\mu$L of MTT (5 mg/mL) was added into each well and incubated for further 4 h. The supernatant then was discarded, and the precipitated MTT formazan was dissolved in 200 $\mu$L of DMSO (dimethyl sulfoxide). The absorbance at 570 nm was measured by Molecular Devices (SpectraMax $M^2e$). Wells without cells were used as blanks, and wells without peptides were taken as negative controls.


DOI: 10.1021/acsami.5b04547
ACS Appl. Mater. Interfaces 2015, 7, 17346−17355

Hemolytic activities of the peptides were studied by using fresh human red blood cells (hBCs). 100 μL of hBCs suspended in PBS at 8% (V/V) was mixed with 100 μL of different peptides with a serial of reduced dilutions by a factor of 2 in a sterile 96-well plate and incubated for 1 h at 37 °C. After centrifuging at 1000*g* for 5 min, 100 μL aliquots of the supernatant were transferred into a new 96-well plate, and hemoglobin release was recorded by the absorbance at 540 nm with Molecular Devices (SpectraMax $M^2e$). Erythrocytes in PBS and in 0.1% Triton X-100 were employed as the negative and positive controls.

**2.6. Locations of G(IIKK)$_3$I-NH$_2$ and (IIKK)$_3$-NH$_2$ in Bacteria and HpeG2 Cells.** For bacteria, FITC-G(IIKK)$_3$I-NH$_2$ and Rhodamine-(IIKK)$_3$-NH$_2$ were added into the wells containing *B. subtilis* 168 ($1\times 10^7$ CFU/mL) at the final concentration of 20 μM for 1 h at 37 °C. The concentrations of the bacteria and peptides used here were both 10 times higher than that used in the antibacterial activity assay to ensure good visualization of the peptide distributions. The samples were centrifuged to remove unbound peptides and were washed three times with PBS. The bacteria were then fixed with 2.5% glutaraldehyde for 1 h, and washed three times. Twenty microliters of bacterial suspensions was immobilized on a glass slide and observed with a Nikon confocal microscope (Nikon C1Si, oil lens). For the images of HpeG2 cells, the cells were preincubated in an eight-well plate for 24 h, and then the cells ($1 \times 10^5$ cells/mL) were washed with PBS and incubated with FITC-G(IIKK)$_3$I-NH$_2$ or Rhodamine-(IIKK)$_3$-NH$_2$ at the concentration of 30 μM, which was near the $IC_{50}$ value (defined as the 50% growth inhibition) of G(IIKK)$_3$I-NH$_2$ against HpeG2 cells, for 1 h at 37 °C under 5% $CO_2$ atmosphere. The cells were washed with PBS three times and observed under a Nikon confocal microscope (Nikon C1Si, 20× lens).

**2.7. Surface Pressure and Association of Peptides into Different Lipid Monolayers.** Surface physical activity of peptides was determined by measuring the surface pressure changes ($\pi$, mN/m) at the air/water interface after injecting the respective peptide into the subphase solution (10 mM Tris-HCl buffer with 154 mM NaCl, pH 7.4). The experiments were done by using a multiwells plate supplied with the Micro trough X instrument (Kibron Inc., Helsinki, Finland). The final concentration of peptides was fixed at 3 μM, and all experiments were carried out at 20 ± 1 °C.

To investigate the penetration ability of peptides into different phospholipid monolayers, various amounts of eggPC, eggPG, eggPC/cholesterol, and eggPG/cholesterol solutions in chloroform were spread at the air/water interface. After 15 min for chloroform evaporation, the peptide was injected into the subphase (10 mM Tris-HCl buffer with 154 mM NaCl, pH 7.4) at the final concentration of 3 μM. Changes of $\pi$ ($\Delta\pi$) were monitored for 30−40 min following the injection of each peptide. All measurements were performed at 20 ± 1 °C.

**2.8. (IIKK)$_3$-NH$_2$ Selectivity between Bacteria and HDFa Cells *in Vitro*.** The selectivity of (IIKK)$_3$-NH$_2$ between bacteria and human normal eukaryotic cells was assessed by the coculture system containing primary human dermal fibroblast (HDFa) cells (Lifeline Cell Technology, FC-0024) and *B. subtilis* 168, and the detailed protocol was described previously.[29] Briefly, Rhodamine-(IIKK)$_3$-NH$_2$ at a final concentration of 20 μM was added into the wells containing the preincubated HDFa cells ($1 \times 10^5$ cells/mL) and bacteria ($1 \times 10^7$ CFU/mL). After incubation for 1 h at 37 °C, the bacteria were collected by centrifuging. Both bacteria and the adhesive HDFa cells were washed with PBS three times. The location of Rhodamine-(IIKK)$_3$-NH$_2$ was observed by using confocal microscopy.

**2.9. *In Vivo* Anti-infection Activity of (IIKK)$_3$-NH$_2$ with a Mouse Peritonitis Model.** The lethal minimum concentration (LMC) that could lead to mice death within 48 h of infection was determined by injecting intraperitoneally various concentrations of *ESBL-E. coli* bacteria (with 0.5 mL volume injection). The LMC was found to be about $5 \times 10^9$ CFU/mL.

After the mice (body weights were about 20 g each) were intraperitoneally injected with 0.5 mL of *ESBL-E. coli* ($5 \times 10^9$ CFU/mL) for 1 h, they were randomly divided into 2 groups, with 5 mice in each group. Group 1 was injected with PBS; group 2 was injected with (IIKK)$_3$-NH$_2$ at a dose of 1.5 mg/kg ((IIKK)$_3$-NH$_2$ was dissolved in PBS). Both PBS and peptide solutions were given by tail vein injection twice a day and lasted for the first 3 days. The number of mice surviving in each group was monitored for up to 14 days after treatment. After 14 days of surveillance, blood samples were collected from the survival mice, and the concentrations of AST (aspartate aminotransferase), ALT (alanine aminotransferase), creatinine, urea nitrogen, and NaCl of the normal (noninfected mice) or peptide treated mice were also tested by ELISA (Enzyme-Linked Immunosorbent Assay).

## 3. RESULTS AND DISCUSSION

**3.1. Peptide Characterizations.** *3.1.1. Peptide Terminal Modifications and Fundamental Properties.* To better understand the effects of N- and C-terminal amino acids on the structural stability and bioactivity of G(IIKK)$_3$I-NH$_2$, we have synthesized a set of peptides by selectively deleting their terminal amino acids. Table 1 lists the four peptide sequences

**Table 1. Fundamental Properties of the Designed Peptides**

| peptide sequences | charges | theoretical molecular weight | observed molecular weight from MS | retention time in RP-HPLC (min) |
|---|---|---|---|---|
| (IIKK)$_3$I-NH$_2$ | +7 | 1578.19 | 1579.2 | 15.2 |
| G(IIKK)$_3$-NH$_2$ | +7 | 1522.08 | 1523.1 | 16.2 |
| G(IIKK)$_3$I-NH$_2$ | +7 | 1635.24 | 1634.4 | 18.5 |
| (IIKK)$_3$-NH$_2$ | +7 | 1465.03 | 1464.3 | 13.0 |

and their fundamental properties. All four peptides contain the same positive charges (+7) at the physiological pH, but they have different hydrophobicity as determined by the retention time in RP-HPLC. The hydrophobicity is in the order: G(IIKK)$_3$I-NH$_2$ > G(IIKK)$_3$-NH$_2$ > (IIKK)$_3$I-NH$_2$ > (IIKK)$_3$-NH$_2$. The molecular weights of these peptides were determined by MALDI-TOF MS, and the results coincided well with the theoretical values, indicating that the products corresponded to the designed sequences (Figure S1).

From the Schiffer−Edmundson wheel drawn, we can see that the four peptides have well-defined helical structures with clear hydrophobic and hydrophilic faces (separated by the dash-dotted red line) (Figure 1). In each case, one lysine is inserted into the hydrophobic isoleucine face, which was thought to help decrease hemolytic activity but has little impact on antibacterial activity.[27,30] The selective incorporation of Gly and Ile at the two termini in the four peptides enables us to examine how different terminal modifications affect the antibacterial and hemolytic activities of the peptide series.

*3.1.2. Secondary Structures.* The CD measurements revealed that all four peptides presented random coil structures in water (Figure 2a), but when mixed into SDS micellar solution they all rearranged into typical α-helix-rich structures characterized by minimal mean molar ellipticity values at 208 and 222 nm (Figure 2b). Considering the helicity of the peptides valued by $\theta_{222}$,[31] it is obvious that G(IIKK)$_3$-NH$_2$ has the minimum helix content while (IIKK)$_3$I-NH$_2$ has the highest helicity among the four peptides. The results indicated that Gly$^1$ in the peptide series disfavored helical structure formation under the membrane-mimic environment, possibly because of its high conformational flexibility. The same effect was observed when Gly$^1$ bearing peptides bounded to lipid bilayers.[21] On the


DOI: 10.1021/acsami.5b04547
ACS Appl. Mater. Interfaces 2015, 7, 17346−17355

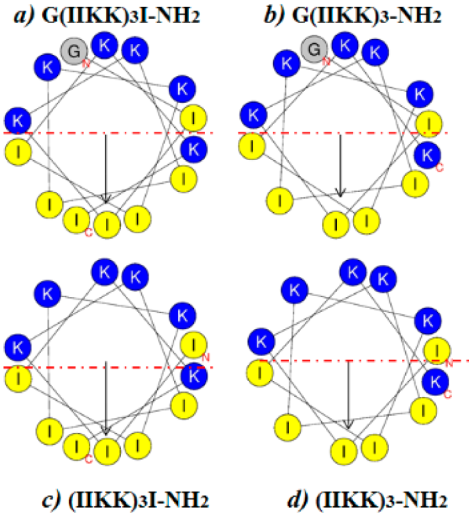


**Figure 1.** Schiffer–Edmundson wheel projection of the four peptides. (a) G(IIKK)$_3$I-NH$_2$, (b) G(IIKK)$_3$-NH$_2$, (c) (IIKK)$_3$I-NH$_2$, and (d) (IIKK)$_3$-NH$_2$. Yellow circles denote hydrophobic amino acids, and blue circles represent hydrophilic amino acids (drawn from the online tool at the Web site: http://heliquest.ipmc.Cnrs.fr/cgi-bin/ComputParams.py).

other hand, the C-terminal isoleucine increased the helicity of (IIKK)$_3$I-NH$_2$ and G(IIKK)$_3$I-NH$_2$. It has been indicated that C-terminal capping motifs were more important for reducing helical contents and some amino acids such as Gly were regarded as a good helix terminating residue at the C-terminal position.[31] Isoleucine, containing the $\beta$-branch of $-CH_3$, was not regarded as a good helix promoting amino acid.[32] However, Ile at the C-terminus ended on the hydrophobic surface and closely interacted with the other Ile residues, which in turn promoted and stabilized the helical structures, as indicated in Figure 1. The balance between the disturbance of Gly$^1$ at the N-terminus and the enhancement of Ile at the C-terminus on the helix structure resulted in an intermediate helicity of G(IIKK)$_3$I-NH$_2$ between (IIKK)$_3$I-NH$_2$ and G(IIKK)$_3$-NH$_2$. When deleting both Gly$^1$ and C-terminal isoleucine, (IIKK)$_3$-NH$_2$ turned out to have the helix content similar to G(IIKK)$_3$I-NH$_2$, suggesting an almost equivalent offset from the two terminal amino acids.

*3.1.3. Surface Properties.* Apart from the secondary structures in different solutions, we also tested the surface adsorption of the peptides by injecting them into the subphase of Tris-HCl buffer containing 154 mM NaCl. The surface pressure changes were measured by surface tension decline from that of the pure water (the $\pi$ values) at the air/water interface. Figure 3a shows a significant increase in $\pi$ upon the injection of each of the peptides into the subphase solution with the final concentration of 3 $\mu$M. All of the peptides demonstrated the trend of tending to the equilibrated $\pi$ values after the first minute of injection (Figure 3 b). The final surface pressures were found to be 15, 12, 9, and 6 mN/m for (IIKK)$_3$I-NH$_2$, G(IIKK)$_3$I-NH$_2$, G(IIKK)$_3$-NH$_2$, and (IIKK)$_3$-NH$_2$, respectively. The order of their surface pressure changes was consistent with the helical contents in SDS solution obtained from the CD spectra as shown in Figure 2b ((IIKK)$_3$I-NH$_2$ > G(IIKK)$_3$I-NH$_2$ > G(IIKK)$_3$-NH$_2$), except for (IIKK)$_3$-NH$_2$, showing that the amphiphilic structures adopted upon adsorption would follow the main trend of the helical structures adopted in incorporation to the SDS micelles. The discrepancy shows that while Gly$^1$ reduces the $\alpha$-helical content, it imposes a subtle influence on the amphiphilic balance, leading to the further reduction of surface tension. In general, surface adsorption and the subsequent surface pressure increase are associated with conformational changes.[33] $\alpha$AMPs tend to fold into amphiphilic helical structures at the interface with the lowest surface energy possible to allow the hydrophilic side groups to be oriented into the subphase and the hydrophobic ones to be projected onto the air side. Similar segment distributions may occur at the curved oil/water interface surrounding the SDS micelles, but given the different interfacial environments, the different orders as observed between some of the peptides are not surprising. On the other hand, it is unclear if the secondary structures adopted at the air/water interface would follow the same order as that for the surface pressure changes due to the lack of experimental capability to determine the secondary structures of the surface adsorbed peptides. Importantly, however, the results imply that all of the peptides studied must have maintained their secondary structures and their amphiphilic characters when adsorbed on the air/water interface. Hence, the strong surface physical activity of AMPs must benefit from a combination of the maintenance of some content of the second structures and amphiphilic performance at the interface. These two features and their interplay would directly implicate their actions to cell membranes. It is therefore useful to try to establish their correlation with antibacterial activity and cytotoxicity to

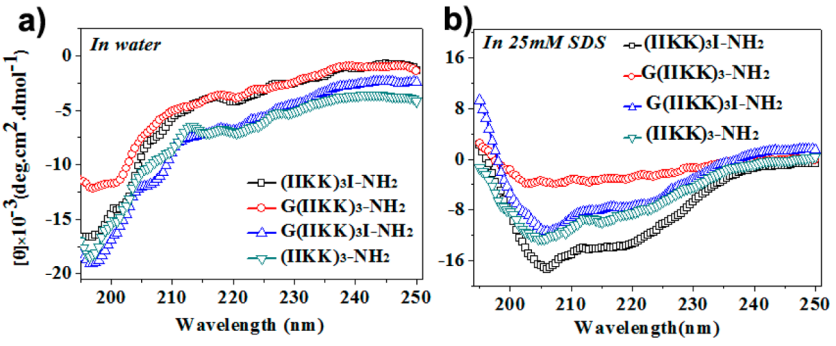


**Figure 2.** CD spectra of the peptides in (a) water and (b) 25 mM SDS aqueous solution. All four peptides present random coil structures (negative peak below 200 nm) in water and adopted helical structures (two negative peaks at 208 and 222 nm, respectively) in the membrane-mimic environment (25 mM SDS). Peptide concentrations were fixed at 0.1 mM, and all measurements were made under ambient temperature of 20–22 °C.


DOI: 10.1021/acsami.5b04547
ACS Appl. Mater. Interfaces 2015, 7, 17346–17355

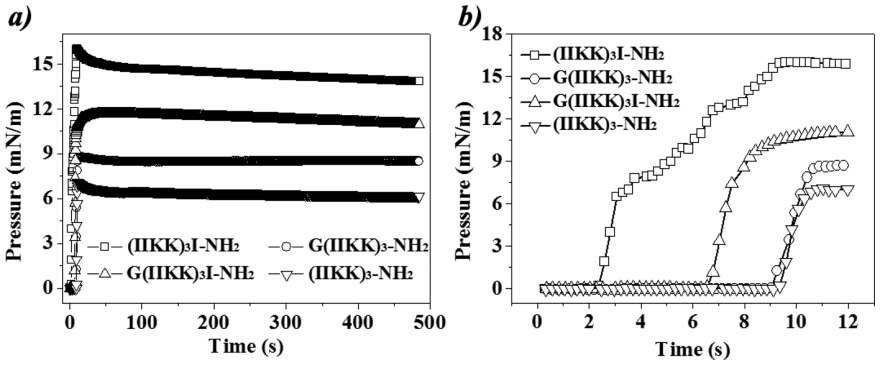


**Figure 3.** (a) Surface physical activity of the four peptides plotted against adsorption time (480 s) measured at the air/water interface. (b) The same surface physical activity of the four peptides measured over the first 12 s upon their injections into the subphase (10 mM Tris-HCl buffer with 154 mM NaCl, pH 7.4). The final concentration of each peptide was 3 $\mu$M.

mammalian host cells, an important assessment of their biological functions.

**3.2. Antibacterial and Antitumor Activity.** *3.2.1. Antibacterial Activity versus Cytotoxicity.* Antibacterial activities of the four peptides against $G^-$ (*E. coli BL21* and *ESBL-E. coli*) and $G^+$ (*B. subtilis* and *S. aureus*) bacteria were investigated by using the standard microdilution method as described previously.[27] The MIC values of the peptides against these bacterial strains were summarized in Table 2. Although all of these peptides showed good antimicrobial activities, there were differences in their MIC values under the test method adopted. Their antibacterial activities were in the order $(IIKK)_3I\text{-}NH_2 \sim G(IIKK)_3I\text{-}NH_2 > G(IIKK)_3\text{-}NH_2 > (IIKK)_3\text{-}NH_2$. It was noted that all peptides were effective against *B. subtilis* with the MIC values between 2.5 and 5 $\mu$M, but less so to *S. aureus* with higher MIC values. The difference may well arise from the different compositions of the bacterial membranes. The trend of increasing MIC values follows that of the surface pressure changes, suggesting that the different bactericidal effects are associated with their different membrane penetrating ability, as to be discussed later.

**Table 2. Antibacterial Activity and Hemolytic Activity of the Designed Peptides**

| | MIC[a] ($\mu$M) | | | | |
|---|---|---|---|---|---|
| peptide sequences | *E. coli BL21* | *ESBL-E. coli* | *B. subtilis* | *S. aureus* | hemolyticity[b] ($\mu$M) hBCs |
| $G(IIKK)_3I\text{-}NH_2$ | 10 | 8 | 5 | 7.5 | 256 |
| $(IIKK)_3I\text{-}NH_2$ | 2.5 | 12 | 5 | 7.5 | 256 |
| $G(IIKK)_3\text{-}NH_2$ | 20 | 20 | 2.5 | 20 | 512 |
| $(IIKK)_3\text{-}NH_2$ | 30 | 20 | 5 | 30 | >1000 |

[a]Minimum inhibitory concentration (MIC) is the lowest concentration of the peptides that will inhibit the visible growth of a microorganism after 18 h incubation. Briefly, the bacteria from the exponential growth phase were washed and incubated with the peptide in serial reduced dilutions by a factor of 2 in a sterile 96-well plate. The bacteria were incubated at 37 °C for 18 h, and the absorbance at 600 nm was recorded. [b]The peptide concentration that lyses 50% hBCs. The fresh hBCs were washed and incubated with different peptides in serial reduced dilutions by a factor of 2 in a sterile 96-well plate and incubated for 1 h at 37 °C, and the hemoglobin release was recorded by the absorbance at 540 nm.

From the results shown in Table 2, it can be seen that deletion of the N-terminal Gly from $G(IIKK)_3I\text{-}NH_2$ had little influence on antibacterial and hemolytic activity, while deletion of the C-terminal Ile decreased its antibacterial performance as evident from the increased MICs. If both of the terminal amino acids were deleted, the antibacterial activity became worsened, but the cytotoxicity toward the normal cells disappeared, even up to the highest hemolytic concentration studied at 1000 $\mu$M.

*3.2.2. Membrane Penetration Ability into Lipid Monolayers.* Our previous study indicated that $G(IIKK)_3I\text{-}NH_2$ killed these bacteria by membrane disruption.[27] Thus, we tested the penetration capability of the four peptides into different lipid monolayers at the molecular level. Monolayers of eggPC, eggPG, eggPC/cholesterol, and eggPG/cholesterol were used to mimic normal mammalian cell and bacterial membranes, respectively.[33−35] Over the concentration ranges studied, the peptides caused a mere increase of the surface pressure by 1−6 mN/m when added into the subphase of the eggPC monolayer (Figure 4a). The final pressure of the monolayer was in the order: $G(IIKK)_3I\text{-}NH_2 > (IIKK)_3I\text{-}NH_2 \sim G(IIKK)_3\text{-}NH_2 > (IIKK)_3\text{-}NH_2$, broadly consistent with the order of their hemolytic activity (Table 2).

On the other hand, all four peptides can substantially increase the surface pressure of the negative eggPG monolayer by 8−10 mN/m (Figure 4b), consistent with their strong responses to bacterial membranes, showing the clear influence of the electrostatic interaction between the positively charged AMPs and the negative bacterial membranes (Table 2). Although the four peptides contained the same positive charges (+7), deleting both terminal amino acids reduced the binding ability to the neutral phospholipid monolayer but not to the negative lipid monolayer. These results together suggested that deleting terminal amino acids can increase the peptides' biocompatibility to host cells without losing their potency in killing bacteria. In many practical applications, however, it is the balance of antibacterial activity and cytotoxicity that must be considered.

Apart from the different charge features of mammalian cells and bacteria, the compositional differences in their cell membranes must also play a role. For example, mammalian cell membranes contain some cholesterol molecules, which tend to increase membrane packing and reduce membrane fluidity. As a result, cholesterol presence may well alter the responses of mammalian cell membranes upon exposure to AMPs.[36] We next tested the penetration of these peptides into the monolayers of eggPC/cholesterol and eggPG/cholesterol


DOI: 10.1021/acsami.5b04547
ACS Appl. Mater. Interfaces 2015, 7, 17346−17355

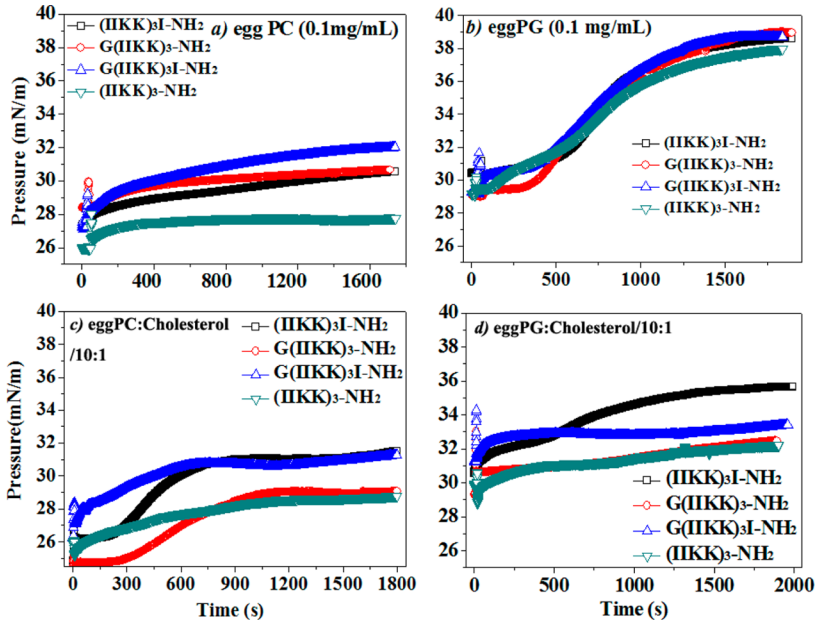


**Figure 4.** Differences in the penetration ability of the four peptides in different lipid monolayers. (a) eggPC, (b) eggPG, (c) eggPC/cholesterol (10:1), and (d) eggPG/cholesterol (10:1). After the formation of different lipid monolayer, each peptide was injected into the subphase of 10 mM Tris-HCl buffer containing 154 mM NaCl at the final concentration of 3 $\mu$M. The changes of the surface pressure were monitored against time.

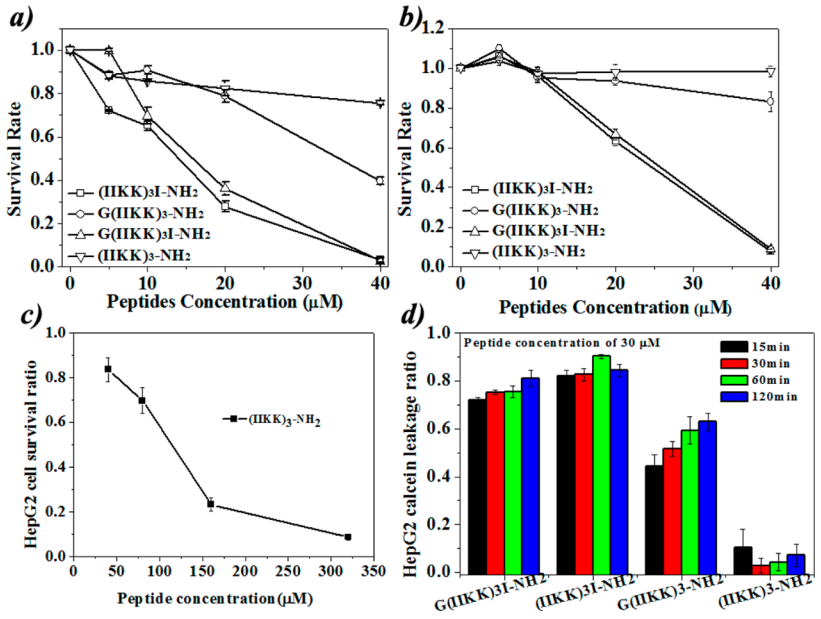


**Figure 5.** Antitumor activities of the four peptides against (a) HeLa and (b) HpeG2 cells by MTT assay. (c) Antitumor activity of $(IIKK)_3$-$NH_2$ against HpeG2 over high concentration range. Briefly, the tumor cells were preincubated for 24 h, and then the peptide was added into the wells. After incubation for 24 h, 20 $\mu$L of MTT was added into the wells for 4 h, the formazan was dissolved in DMSO, and the absorbance at 570 nm was recorded. Cell survival rate was calculated as compared to the controls. (d) Calcein release from HpeG2 cells treated with different peptides for 15, 30, 60, and 120 min, respectively. The preincubated HpeG2 cells were stained with calcein-AM for 30 min in the dark, and then each peptide was added into the wells at a concentration of 30 $\mu$M and incubated for different intervals. The fluorescence of the supernatant was tested, and the calcein release was calculated as compared to the control samples.

(w/w, 10:1). Figure 4c shows that the presence of cholesterol has little effect on the interaction between the peptides and neutral eggPC/cholesterol monolayer. The increase of the surface pressure was broadly similar to that without cholesterol (Figure 4a and c). However, the presence of cholesterol decreased the penetration ability of all of the peptides into the eggPG/cholesterol monolayer (Figure 4b and d). Among these four peptides, $(IIKK)_3$I-$NH_2$ had the highest penetration ability into the eggPG/cholesterol monolayer, and the final surface pressure was about 36 mN/m, slightly lower than that of the eggPG monolayer alone. In contrast, injection of 3 $\mu$M $(IIKK)_3$-$NH_2$ into the subphase of the eggPG/cholesterol monolayer led to only about a 3 mN/m increase of the surface pressure (from 29 to 32 mN/m). This was compared to the increase of about 8 mN/m of surface pressure in eggPG monolayer alone (Figure 4b), suggesting that cholesterol


DOI: 10.1021/acsami.5b04547
ACS Appl. Mater. Interfaces 2015, 7, 17346−17355

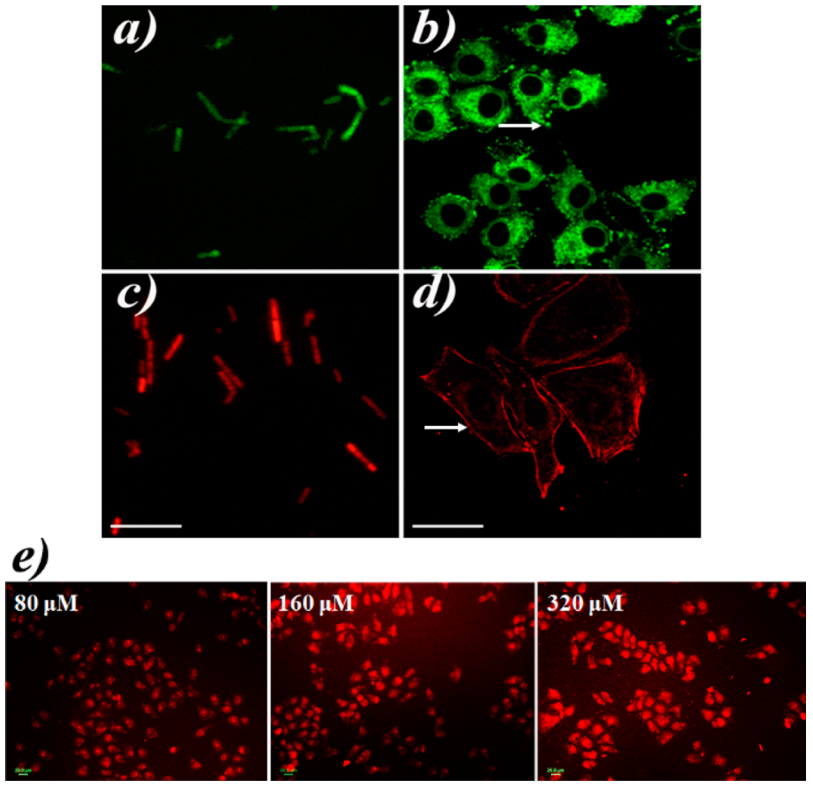


**Figure 6.** Locations of FITC-G(IIKK)$_3$I-NH$_2$ and Rhodamine-(IIKK)$_3$-NH$_2$ in *B. subtilis* 168 (a and c) and HpeG2 cells (b and d). After incubation with peptides at a concentration of 20 $\mu$M for 1 h at 37 °C in the dark, the bacteria ($1 \times 10^7$ CFU/mL) were collected and washed three times, and then the peptide locations were observed under fluorescence microscopy (a and c). For HpeG2 cells, the peptides at a concentration of 30 $\mu$M were added into the wells containing the preincubated cells and incubated for 1 h at 37 °C in the dark, and the locations of peptides in the cells were observed under fluorescence microscopy (b and d). (e) The locations of Rhodamine-(IIKK)$_3$-NH$_2$ in HpgG2 cells at different peptide concentrations. Bar = 20 $\mu$m.

existence in the membrane strongly inhibited the penetration ability of (IIKK)$_3$-NH$_2$. These differences would have implications on their anticancer potency as mammalian cell membranes usually contain cholesterol molecules.

*3.2.3. Antitumor Activity.* Different penetration abilities into eggPG/cholesterol monolayers may imply that these peptides have different antitumor activities. To test this hypothesis, we examined the antitumor activities of the four peptides by using HeLa (derived from human cervical cancer tissue) and HpeG2 (derived from malignant human liver tissue) cells (Figure 5a and b). Consistent with the penetration capacities into eggPG/cholesterol monolayers, (IIKK)$_3$I-NH$_2$ and G(IIKK)$_3$I-NH$_2$ had high antitumor activities. The IC$_{50}$ values were about 16 $\mu$M against HeLa cells and 25 $\mu$M against HpeG2 cells. Figure 5d shows the membrane disruption versus incubation time of the four peptides against HpeG2 cells. For G(IIKK)$_3$I-NH$_2$ and (IIKK)$_3$I-NH$_2$, over 80% cells were disrupted within the first 15 min at the concentration of 30 $\mu$M, showing that the interactions with cell membranes were sufficiently fast. For G(IIKK)$_3$-NH$_2$, there was a slow release of calcein from HpeG2 cells, indicating that more G(IIKK)$_3$-NH$_2$ molecules were needed to disrupt the membrane. (IIKK)$_3$-NH$_2$ did not cause much inhibition of the tumor cells at the concentration as high as 30 $\mu$M, and the calcein leakage of HpeG2 cells could not be observed at this peptide concentration either (Figure 5d). The low surface activity and weak penetration into the eggPG/cholesterol monolayers suggest that more (IIKK)$_3$-NH$_2$ molecules were needed to drive the peptide into the HpeG2 cell membranes to overcome the obstacle of cholesterol. We then tested the antitumor activity of (IIKK)$_3$-NH$_2$ over the higher concentration range by extending it to 340 $\mu$M. The results showed that the IC$_{50}$ value against HpeG2 was about 120 $\mu$M and that all of the HpeG2 cells would actually be killed at concentrations around 340 $\mu$M (Figure 5c).

*3.2.4. Location of G(IIKK)$_3$I-NH$_2$ and (IIKK)$_3$-NH$_2$ in Bacteria and Tumor Cells.* Similar penetration abilities of G(IIKK)$_3$I-NH$_2$ and (IIKK)$_3$-NH$_2$ into the negative eggPG monolayer corroborated well with their comparable antibacterial activities, suggesting similar membrane disruptive interactions initiated by both peptides. However, the existence of cholesterol in the eggPG monolayer greatly decreased the penetration ability of (IIKK)$_3$-NH$_2$, but it had less influence on G(IIKK)$_3$I-NH$_2$. This difference has also shown remarkable consistency with their different inhibition potencies against the two cancerous cells, thus again pointing to the selective actions to the membranes containing cholesterol. To confirm the different interactions of the two peptides with bacterial and tumor cell membranes, we attempted to observe the locations of G(IIKK)$_3$I-NH$_2$ and (IIKK)$_3$-NH$_2$ in bacteria (*B. subtillis* 168) and tumor cells (HpeG2) by using two fluorescent tag labeled peptides. FITC-G(IIKK)$_3$I-NH$_2$ and Rhodamine-(IIKK)$_3$-NH$_2$ emit green and red lights upon excitation by blue or yellow lights, respectively. Both peptides were incubated with *B. subtilis* 168 and then observed by fluorescence microscopy. As evident in Figure 6a and c, green and red fluorescent colors are clearly visible inside the bacteria, indicating the disruption of bacterial membranes and the subsequent internalization of the peptides.


DOI: 10.1021/acsami.5b04547
ACS Appl. Mater. Interfaces 2015, 7, 17346−17355

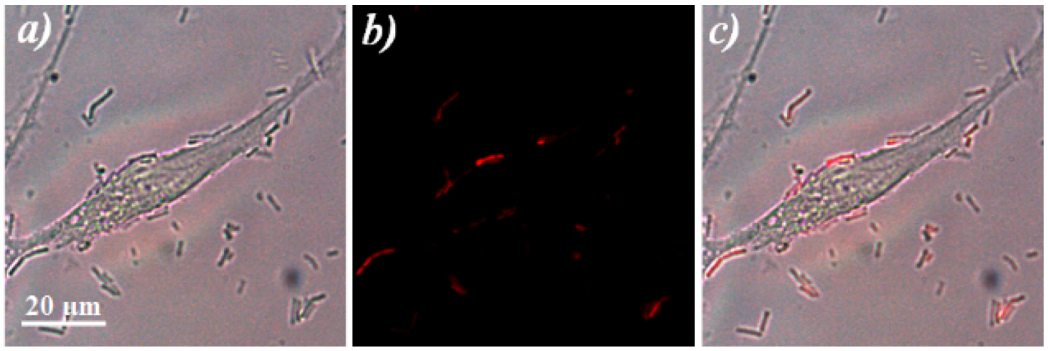


**Figure 7.** Cell selectivity of $(IIKK)_3$-$NH_2$ in the coculture system containing *B. subtilis* 168 (rods) and HDFa (spindles) (bar = 20 $\mu$m). HDFa cells were preincubated in an eight-well plate, and then the bacteria was added into the wells containing the cells. Rhodamine-$(IIKK)_3$-$NH_2$ at a concentration of 20 $\mu$M was added into the wells and incubated for 1 h at 37 °C in the dark. Peptide locations were observed by fluorescence microscopy. (a) Black and white field; (b) the same field observed under fluorescence microscopy; and (c) overlay of (a) and (b).

On the other hand, the locations of the two peptides in HpeG2 cells showed clear peptide-dependent processes and were thus different from those observed from the bacteria (Figure 6b and d). The green fluorescence emitted by FITC-$G(IIKK)_3I$-$NH_2$ was accumulated inside HpeG2 cells, indicating the translocation of the peptide across the phospholipid bilayers. During this process, the interaction with the peptide would result in the gradual structural deterioration of the cell membranes. As a result, the cells became thin and the cell boundary became blurry (Figure 6b, arrow). In contrast, we can see a clearly red cell boundary excited by Rhodamine-$(IIKK)_3$-$NH_2$, suggesting that $(IIKK)_3$-$NH_2$ was mostly localized inside the cell membranes (Figure 6d, arrow). The cells treated with Rhodamine-$(IIKK)_3$-$NH_2$ were flat, and the microvilli are clearly visible. Obviously, some polarized clusters could also be observed around the cells, suggesting that the interactions between $(IIKK)_3$-$NH_2$ and the cell membranes caused some morphological stimulations but have not lyzed the cell membranes. However, more $(IIKK)_3$-$NH_2$ molecules were found inside the cells when increasing the peptide concentration (Figure 6e), indicating that $(IIKK)_3$-$NH_2$ could disrupt HpeG2 cell membranes and become internalized if the peptide concentration reached a certain threshold.

**3.3. Selectivity of $(IIKK)_3$-$NH_2$ *in Vitro* from Cell Coculturing and *in Vivo* from Mouse Model.** The above cancerous HpeG2 cell studies show that $(IIKK)_3$-$NH_2$ had to work at rather high concentrations and would not seem to be ideal for antitumor treatment. However, its high antibacterial activity with low toxicity to normal mammalian cells made it highly attractive to the treatment of some of the bacterial infections. We thus tested its selectivity against bacteria and human dermal fibroblasts (HDFa) through a coculture system *in vitro*. Rhodamine-$(IIKK)_3$-$NH_2$ was added into the coculture system containing both *B. subtilis* 168 and HDFa, and peptide locations were visualized by confocal microscopy after incubation for 1 h. As shown in Figure 7b, the red fluorescence of Rhodamine-$(IIKK)_3$-$NH_2$ was concentrated in the bacteria but not in the primary HDFa cells. Similar results were also obtained for FITC-$G(IIKK)_3I$-$NH_2$ in the coculture system containing both *B. subtilis* 168 and HDFa.[29] The results confirmed that both $(IIKK)_3$-$NH_2$ and $G(IIKK)_3I$-$NH_2$ can respond fast and effectively recognize pathogenic bacteria at low concentration (20 $\mu$M) in the coculture system mimicking the *in vivo* infected environment.

*ESBL*-producing bacteria are widely known to be resistant to many antibiotics and have caused numerous threats to public health.[37] On the basis of the studies as reported above, we have further examined the antimicrobial activities of $(IIKK)_3$-$NH_2$ *in vivo*. It was found that injection of *ESBL-E. coli* bacteria into mice intraperitoneally (about $5 \times 10^9$ CFU/mL, 0.5 mL injection volume) could cause mice death within 48 h. After the mice were infected for 1 h with this fixed amount of bacterial injection, the peptide solution was injected by tail vein at the doses of 1.5 mg/kg twice per day for the first 3 days. The *ESBL-E. coli* infected mice treated with PBS were used as negative control, and they all died from the first few hours to some 20 h following injection with the bacteria. In contrast, injection of $(IIKK)_3$-$NH_2$ six times over the first 3 day period saved 80% mice at the end of 14 days, showing its clear efficacy against *ESBL-E. coli* bacteria *in vivo* (Table 3). The concentrations of AST, ALT, creatinine, urea nitrogen, and NaCl in the blood of the normal (control) or peptide treated mice were also examined. The results (Table 3) showed that there were no significant differences of these tested molecules between PBS or peptide treatment from the noninfected mice (control), suggesting that injection of the peptides at the dose of 1.5 mg/kg did not harm the major organs of mice such as liver and kidney.

**Table 3. Survival Rates and Related Molecular Characterization Parameters after the Treatment of $(IIKK)_3$-$NH_2$ in the Mouse Model[a]**

| samples | control | PBS | 1.5 mg/kg |
|---|---|---|---|
| survival rate | 100% | 0 | 80% |
| ALT (U/L) | 29.0 ± 1.2 | 30.6 ± 1.4 | 32.3 ± 0.7 |
| AST (U/L) | 65.2 ± 1.5 | 66.6 ± 2.3 | 70.2 ± 1.9 |
| creatinine ($\mu$M) | 18.2 ± 1.1 | 18.6 ± 0.7 | 18.3 ± 1.0 |
| urea nitrogen (mM) | 4.7 ± 0.5 | 4.5 ± 0.5 | 4.2 ± 0.6 |
| NaCl (mM) | 126.9 ± 4.3 | 128.1 ± 5.8 | 124.1 ± 7.3 |

[a]*ESBL-E. coli* ($5 \times 10^9$ CFU/mL) infected mice were treated with PBS or $(IIKK)_3$-$NH_2$ at a dose of 1.5 mg/kg. After treatment, the number of mice surviving in each group was monitored for up to 14 days, and then blood samples from the survival mice were collected for testing the concentrations of AST, ALT, creatinine, urea nitrogen, and NaCl. Control samples were collected from the normal mice (no infection).

## 4. CONCLUSION

The impact of N- and C-terminal modifications of a well-characterized $\alpha$AMP $G(IIKK)_3I$-$NH_2$ on its selective responses to model membranes and antibacterial and anticancer


DOI: 10.1021/acsami.5b04547
ACS Appl. Mater. Interfaces 2015, 7, 17346−17355

bioactivities *in vitro* and *in vivo* has been carefully examined. We have focused on assessing the effects of deletions of Gly on the N-terminus and Ile on the C-terminus on the helical structures of the peptide series under different conditions, their membrane lytic interactions, and selective cell responses to the coculture containing bacteria and primary human skin fibroblast cells. It was found that the N-terminal Gly reduced the helical structure formation of $G(IIKK)_3$-$NH_2$, while the C-terminal Ile improved the helical conformation of $(IIKK)_3I$-$NH_2$. When the two amino acids were absent at the respective terminals, the helical content of $(IIKK)_3$-$NH_2$ was found to be similar to that of $G(IIKK)_3I$-$NH_2$, indicating the counterbalancing of the opposite effects from Gly and Ile. All four peptides displayed similar and high penetration capability into eggPG monolayers, leading to their high antibacterial activities against different bacterial strains. This observation suggests the combined effect of the electrostatic driving force and the subsequent hydrophobic association on the structural disruption of the bacterial membranes. In contrast, the C-terminal Ile enhanced the penetrating activity of the peptides into the model eggPG/cholesterol monolayer. As a result, both $(IIKK)_3I$-$NH_2$ and $G(IIKK)_3I$-$NH_2$ showed high antitumor activity against both HeLa and HpeG2 cells. However, the other two peptides without Ile at the C terminal had much lower antitumor activities. Their decreased antitumor performances are well consistent with their low surface pressure increases at the air/water interface and weak penetration abilities into the eggPG/cholesterol monolayer. Although $(IIKK)_3$-$NH_2$ had rather low antitumor activity, its low toxicity to the normal mammalian cells and high antibacterial activity *in vitro* and *in vivo* rendered it a good antibacterial agent.

## ■ ASSOCIATED CONTENT

### Supporting Information

The Supporting Information is available free of charge on the ACS Publications website at DOI: 10.1021/acsami.5b04547.

MALDI-TOF MS of the four peptides used in this work (PDF)

## ■ AUTHOR INFORMATION


### Corresponding Authors

*Tel.: (+86)532-8698-1569. E-mail: xuh@upc.edu.cn.
*Tel.: (+44)-161-200-3926. E-mail: j.lu@manchester.ac.uk.


### Notes

The authors declare no competing financial interest.

## ■ ACKNOWLEDGMENTS

This work was supported by the National Natural Science Foundation of China under grant numbers 31271497, 21373270, and 30900765, the Fundamental Research Funds for the Central Universities (12CX04052A and 14CX02189A). H.X. acknowledges support by the Program for New Century Excellent Talents in University (NCET-11-0735). We thank the UK Engineering and Physical Sciences Research Council (EPSRC) and Technology and Strategy Board (TSB) for support. We also thank Professor Xiaoxing Luo for donating the *ESBL-E. coli* to this research work.

## ■ REFERENCES


(1) Lewis, K. Platforms for Antibiotic Discovery. *Nat. Rev. Drug Discovery* **2013**, *12*, 371−387.
(2) Wright, G. D. Molecular Mechanisms of Antibiotic Resistance. *Chem. Commun.* **2011**, *47*, 4055−4061.
(3) Deris, J. B.; Kim, M.; Zhang, Z.; Okano, H.; Hermsen, R.; Groisman, A.; Hwa, T. The Innate Growth Bistability and Fitness Landscapes of Antibiotic-Resistant Bacteria. *Science* **2013**, *342*, 1237435.
(4) Mookherjee, N.; Hancock, R. Cationic Host Defence Peptides: Innate Immune Regulatory Peptides as a Novel Approach for Treating Infections. *Cell. Mol. Life Sci.* **2007**, *64*, 922−933.
(5) Brogden, K. A. Antimicrobial Peptides: Pore Formers or Metabolic Inhibitors in Bacteria? *Nat. Rev. Microbiol.* **2005**, *3*, 238−250.
(6) Oren, Z.; Shai, Y. Mode of Action of Linear Amphipathic α-Helical Antimicrobial Peptides. *Biopolymers* **1998**, *47*, 451−463.
(7) Hoskin, D. W.; Ramamoorthy, A. Studies on Anticancer Activities of Antimicrobial Peptides. *Biochim. Biophys. Acta, Biomembr.* **2008**, *1778*, 357−375.
(8) Zelezetsky, I.; Tossi, A. Alpha-Helical Antimicrobial Peptides-Using a Sequence Template to Guide Structure-Activity Relationship Studies. *Biochim. Biophys. Acta, Biomembr.* **2006**, *1758*, 1436−1449.
(9) Rotem, S.; Mor, A. Antimicrobial Peptide Mimics for Improved Therapeutic Properties. *Biochim. Biophys. Acta, Biomembr.* **2009**, *1788*, 1582−1592.
(10) Fjell, C. D.; Hiss, J. A.; Hancock, R. E.; Schneider, G. Designing Antimicrobial Peptides: Form Follows Function. *Nat. Rev. Drug Discovery* **2011**, *11*, 37−51.
(11) Braunstein, A.; Papo, N.; Shai, Y. *In vitro* Activity and Potency of an Intravenously Injected Antimicrobial Peptide and Its DL Amino Acid Analog in Mice Infected with Bacteria. *Antimicrob. Agents Chemother.* **2004**, *48*, 3127−3129.
(12) Shai, Y. From Innate Immunity to *De novo* Designed Antimicrobial Peptides. *Curr. Pharm. Des.* **2002**, *8*, 715−725.
(13) Papo, N.; Shai, Y. Host Defense Peptides as New Weapons in Cancer Treatment Cell. *Cell. Mol. Life Sci.* **2005**, *62*, 784−790.
(14) Brogden, N. K.; Brogden, K. A. Will New Generations of Modified Antimicrobial Peptides Improve Their Potential as Pharmaceuticals? *Int. J. Antimicrob. Agents* **2011**, *38*, 217−225.
(15) Findlay, B.; Zhanel, G. G.; Schweizer, F. Cationic Amphiphiles, a New Generation of Antimicrobials Inspired by the Natural Antimicrobial Peptide Scaffold. *Antimicrob. Agents Chemother.* **2010**, *54*, 4049−4058.
(16) Juretić, D.; Vukičević, D.; Petrov, D.; Novković, M.; Bojović, V.; Lučić, B.; Ilić, N.; Tossi, A. Knowledge-Based Computational Methods for Identifying or Designing Novel, Non-Homologous Antimicrobial Peptides. *Eur. Biophys. J.* **2011**, *40*, 371−385.
(17) Ong, Z. Y.; Wiradharma, N.; Yang, Y. Y. Strategies Employed in the Design and Optimization of Synthetic Antimicrobial Peptide Amphiphiles with Enhanced Therapeutic Potentials. *Adv. Drug Delivery Rev.* **2014**, *78*, 28−45.
(18) Nguyen, L. T.; Chau, J. K.; Perry, N. A.; De Boer, L.; Zaat, S. A.; Vogel, H. J. Serum Stabilities of Short Tryptophan and Arginine-Rich Antimicrobial Peptide Analogs. *PLoS One* **2010**, *5*, e12684.
(19) Azad, M. A.; Huttunen-Hennelly, H. E. K.; Ross Friedman, C. Bioactivity and the First Transmission Electron Microscopy Immunogold Studies of Short *De novo*-Designed Antimicrobial Peptides. *Antimicrob. Agents Chemother.* **2011**, *55*, 2137−2145.
(20) Nielsen, S. L.; Frimodt-Møller, N.; Kragelund, B. B.; Hansen, P. R. Structure-Activity Study of the Antibacterial Peptide Fallaxin. *Protein Sci.* **2007**, *16*, 1969−1976.
(21) Gray, C.; Tatulian, S. A.; Wharton, S. A.; Tamm, L. K. Effect of the N-Terminal Glycine on the Secondary Structure, Orientation, and Interaction of the Influenza Hemagglutinin Fusion Peptide with Lipid Bilayers. *Biophys. J.* **1996**, *70*, 2275−2286.
(22) Blondelle, S. E.; Houghten, R. A. Hemolytic and Antimicrobial Activities of the Twenty-Four Individual Omission Analogs of Melittin. *Biochemistry* **1991**, *30*, 4671−4678.
(23) Schmidtchen, A.; Pasupuleti, M.; Mörgelin, M.; Davoudi, M.; Alenfall, J.; Chalupka, A.; Malmsten, M. Boosting Antimicrobial

Peptides by Hydrophobic Oligopeptide End Tags. *J. Biol. Chem.* **2009**, *284*, 17584−17594.
(24) Park, C. B.; Yi, K. S.; Matsuzaki, K.; Kim, M. S.; Kim, S. C. Structure-Activity Analysis of Buforin II, a Histone H2A-Derived Antimicrobial Peptide: The Proline Hinge Is Responsible for the Cell-Penetrating Ability of Buforin II. *Proc. Natl. Acad. Sci. U. S. A.* **2000**, *97*, 8245−8250.
(25) Park, I. Y.; Cho, J. H.; Kim, K. S.; Kim, Y. B.; Kim, M. S.; Kim, S. C. Helix Stability Confers Salt Resistance Upon Helical Antimicrobial Peptides. *J. Biol. Chem.* **2004**, *279*, 13896−13901.
(26) Wiradharma, N.; Khan, M.; Yong, L. K.; Hauser, C. A.; Seow, S. V.; Zhang, S.; Yang, Y. Y. The Effect of Thiol Functional Group Incorporation into Cationic Helical Peptides on Antimicrobial Activities and Spectra. *Biomaterials* **2011**, *32*, 9100−9108.
(27) Hu, J.; Chen, C.; Zhang, S.; Zhao, X.; Xu, H.; Zhao, X.; Lu, J. Designed Antimicrobial and Antitumor Peptides with High Selectivity. *Biomacromolecules* **2011**, *12*, 3839−3843.
(28) Chen, C.; Hu, J.; Zeng, P.; Pan, F.; Yaseen, M.; Xu, H.; Lu, J. Molecular Mechanisms of Anticancer Action and Cell Selectivity of Short α-Helical Peptides. *Biomaterials* **2014**, *35*, 1552−1561.
(29) Chen, C.; Hu, J.; Zeng, P.; Chen, Y.; Xu, H.; Lu, J. High Cell Selectivity and Low-Level Antibacterial Resistance of Designed Amphiphilic Peptide $G(IIKK)_3I\text{-}NH_2$. *ACS Appl. Mater. Interfaces* **2014**, *6*, 16529−16536.
(30) Wiradharma, N.; Sng, M.; Khan, M.; Ong, Z. Y.; Yang, Y. Y. Rationally Designed α-Helical Broad-Spectrum Antimicrobial Peptides with Idealized Facial Amphiphilicity. *Macromol. Rapid Commun.* **2013**, *34*, 74−80.
(31) Huttunen-Hennelly, H. E. An Investigation into the N- and C-Capping Effects of Glycine in Cavitand-Based Four-Helix Bundle Proteins. *Bioorg. Chem.* **2010**, *38*, 98−107.
(32) Nick Pace, C.; Martin Scholtz, J. A Helix Propensity Scale Based on Experimental Studies of Peptides and Proteins. *Biophys. J.* **1998**, *75*, 422−427.
(33) Maget-Dana, R. The Monolayer Technique: A Potent Tool for Studying the Interfacial Properties of Antimicrobial and Membrane-Lytic Peptides and Their Interactions with Lipid Membranes. *Biochim. Biophys. Acta, Biomembr.* **1999**, *1462*, 109−140.
(34) Brockman, H. Lipid Monolayers: Why Use Half a Membrane to Characterize Protein-Membrane Interactions? *Curr. Opin. Struct. Biol.* **1999**, *9*, 438−443.
(35) Alves, I. D.; Bechara, C.; Walrant, A.; Zaltsman, Y.; Jiao, C. Y.; Sagan, S. Relationships between Membrane Binding, Affinity and Cell Internalization Efficacy of a Cell-Penetrating Peptide: Penetratin as a Case Study. *PLoS One* **2011**, *6*, e24096.
(36) Prenner, E. J.; Lewis, R. N.; Jelokhani-Niaraki, M.; Hodges, R. S.; McElhaney, R. N. Cholesterol Attenuates the Interaction of the Antimicrobial Peptide Gramicidin S with Phospholipid Bilayer Membranes. *Biochim. Biophys. Acta, Biomembr.* **2001**, *1510*, 83−92.
(37) Paterson, D. L.; Bonomo, R. A. Extended-Spectrum β-Lactamases: A Clinical Update. *Clin. Microbiol. Rev.* **2005**, *18*, 657−686.


DOI: 10.1021/acsami.5b04547
*ACS Appl. Mater. Interfaces* 2015, 7, 17346−17355